Note: A 102 dB dynamic-range charge-sampling readout for ionizing particle/radiation detectors based on an application-specific integrated circuit (ASIC)

A. Pullia, F. Zocca, and S. Capra

Articles you may be interested in

Note: A 102 dB dynamic-range charge-sampling readout for ionizing particle/radiation detectors based on an application-specific integrated circuit (ASIC)

A. Pullia,[1,2,a)] F. Zocca,[1,2] and S. Capra[1,2]
[1]*Department of Physics, University of Milano, Via Celoria 16, I-20133 Milano, Italy*
[2]*INFN Milano, Via Celoria 16, I-20133 Milano, Italy*

An original technique for the measurement of charge signals from ionizing particle/radiation detectors has been implemented in an application-specific integrated circuit form. The device performs linear measurements of the charge both within and beyond its output voltage swing. The device features an unprecedented spectroscopic dynamic range of 102 dB and is suitable for high-resolution ion and X-γ ray spectroscopy. We believe that this approach may change a widespread paradigm according to which no high-resolution spectroscopy is possible when working close to or beyond the limit of the preamplifier's output voltage swing. *Published by AIP Publishing.* https://doi.org/10.1063/1.5012081

A new CMOS charge-sensitive amplifier for semiconductor detectors of ionizing particles and radiations has been designed and realized, which implements an original fast-reset mode spectroscopy technology aimed at improving the measurement dynamic range and at reducing the dead time due to saturation. This note is focused on this promising technology and its integrated implementation. Using such a technique, the realized front end features a spectroscopy-grade dynamic range of 102 dB which, to the best of our knowledge, is the largest ever for the class of integrated devices for charge measurement. A broad range of applications are foreseen in biomedical imaging, nuclear/sub-nuclear physics experiments, environmental monitoring in the case of radionuclide contamination, and astrophysical experiments.

The working principle of the proposed application-specific integrated circuit (ASIC) has been previously proved with a discrete component circuit,[1] as illustrated in Fig. 1, where the spectrum is shown of an AmBe γ-ray source[2] as obtained using a prototype read-out circuit in the fast-reset mode. In this discrete-component solution[3–5] inspired by older non-integrated circuit structures,[6–8] the fast-reset circuitry is located in the second stage of the electronic chain, and the limiting factor for the dynamic range is the output voltage swing of the first stage, in the order of 12 V. In integrated circuits, however, such a large voltage swing is typically unavailable. We so developed a new technical solution where the fast-reset circuitry is located in the very first stage of the integrated device. This solution yields more than an order of magnitude boost in the ASIC measurement dynamic range, which we believe is an important step forward in this context, and opens the way towards the design of ultra-wide range integrated VLSI front-ends[9–13] for semiconductor detectors.

In Fig. 2(a), a simplified schematic diagram of the detector-preamplifier system is shown. The detector, represented by capacitance C_D, consists of a reverse-biased diode which provides, when hit by an ionizing particle or photon, signal charge Q used to measure the energy of the particle/photon on the basis of the energy-to-charge conversion factor of the detector. The preamplifier basically consists of:

(i) an active integrator which turns the detector charge signal Q into an output voltage V_{OUT} through feedback capacitance C_F. Slow dissipation of Q through external GΩ feedback resistor R_F or through the reverse-biased gate-to-source junction of external JFET J1 is negligible in the typical measurement time scale of a few μs,

(ii) a wrap around time-variant circuit path T1, S, I_R, used for implementing the mentioned fast-reset mode, which provides an optional strong discharge path able to remove Q from node X in a few μs, when needed. This is the hardware part we propose to make the new measurement technique feasible in practice.

Overall the circuit works as a conventional continuous time reset charge preamplifier, based on the circuit structure (i), for detector signals below a given threshold or as a peculiar pulsed-reset charge preamplifier, based on the circuit path (ii), for larger signals.

We will first describe in detail the fast-reset mode and its implementation, and later we will comment on the active integrator. Eventually we will show the obtained experimental results.

As can be seen in Fig. 2(a), the fast-reset device consists of a gated ultra-stable constant-current sink I_R able to drain charge at a constant rate out of the input node X over a proper time window and a Schmitt trigger comparator used to provide the gate signal. The gated current sink is implemented by a CMOS single-pole double-throw switch S and a conventional high quality constant current sink I_R. S is controlled by Schmitt trigger T1, which continuously monitors the output voltage level. T1's thresholds are set respectively at the quiescent output voltage value ~0 V and at a large negative voltage value close to the negative limit of the output voltage swing.

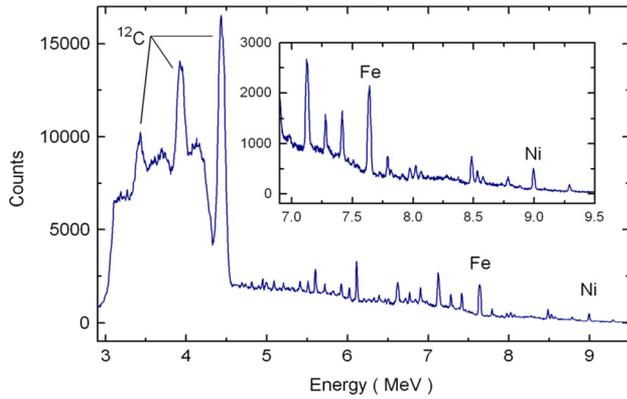a)Author to whom correspondence should be addressed: alberto.pullia@mi.infn.it

FIG. 1. An AmBe γ-ray source is read with a Ge detector and a discrete-component preamplifier implementing the fast-reset technology.

This path is made active whenever V_{OUT} overcomes the latter threshold, i.e., when Q is large enough to put the preamplifier close to or in saturation. When this path is activated, the physical charge trapped in node X gets drained away by the constant current I_R until the output voltage reaches back the quiescent value, T1 commutes and the fast-reset cycle gets automatically interrupted. As a result, the width ΔT of T1's output signal (V_{CMP}) is an indirect reliable linear measurement of Q, according to the definition of electric current,

$$Q = \Delta T \times I_R. \tag{1}$$

Note that I_R should be constant along all discharge transient in order to use Eq. (1) to derive Q. So, accurateness and stability of the constant current sink is paramount in this device. In Eq. (1), we have neglected the contribution of R_F to charge removal, which is typically of the order of 0.1% on a
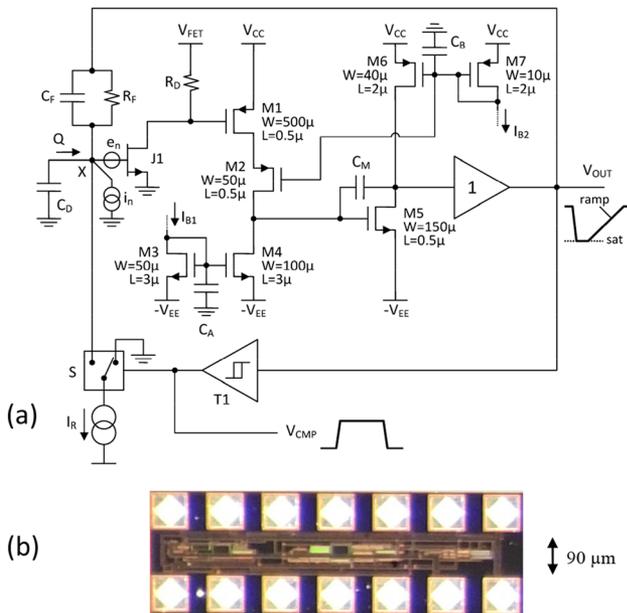

FIG. 2. (a) Schematic diagram of the new integrated device implementing the fast-reset mode technology and (b) micro-photograph of the ASIC. J1, C_F, and R_F are external devices in this implementation. A large Q yields output signal saturation and single-ramp recovery. A rectangular comparator signal is delivered, the width of which is proportional to Q.

time scale of 1 μs. It is worth pointing out that linear relation (1) holds even when Q is so large to put the preamplifier in soft or deep saturation, provided that no additional parasitic discharge path builds up along the measurement cycle. This measurement approach fails only if Q is so large to change substantially the voltage at node X so as to put the gate-to-source junction of J1 in the forward mode. This would open a path to ground for the charge and destroy the physical signal to be measured. But in practice, this is an extremely rare condition in spectrometers based on large p-i-n diodes or HPGe (High-Purity Germanium) detectors, which may occur only in the case of heavy-ion multiple hits.

In Fig. 2(a), an output signal is shown for the case when an over-threshold signal is delivered, so large as to put the preamp into saturation. So, the shape of the output signal flattens up at the beginning. Charge removal from node X along the I_R path begins upon signal arrival and is effective even when the preamp is saturated. When enough charge is removed, the preamp exits from saturation, node X behaves as a virtual ground, and I_R entirely flows through C_F, which yields an output ramp signal. Overall the output signal has a trapezoidal shape. The width ΔT of such trapezoidal signal, which coincides with the width of comparator signal V_{CMP}, is proportional to Q according to Eq. (1).

Note that even if the proposed technique is inspired to the concept of single-ramp Wilkinson's ADC's in this case, any non-linearity or temperature sensitivity of the capacitors involved does not affect the measurement of Q as no capacitive term is present in Eq. (1).

As an issue, it must be said that the fast-reset mode features a large enough signal-to-noise ratio only for relatively large signals. So, the value of the preset threshold point must be chosen carefully depending on the noise specifications of the specific application. For under-threshold signals, the fast-reset mode is not active and the measurement may be performed on a conventional low-noise philosophy basis, using pulse shaping, baseline restoration, and pulse height analysis.[14] Combining the two working modes, the mentioned ultra-wide linear-measurement dynamic range is obtained, with no sacrifice in terms of signal-to-noise ratio.

The circuit architecture of the active integrator, as shown in Fig. 2(a), is straightforward. It consists of a gain amplifier with a feedback path through C_F R_F. The gain amplifier includes a common-source JFET-based input stage (J1) followed by a P-MOS cascade amplifier (M1, M2) and a N-MOS common-source gain stage with Miller capacitance setting the dominant pole of the circuit (M5, C_M). A modified White follower (not shown in detail) is used as output stage. In our prototype device, a few external components are used, including R_F, R_D, J1 (BF862), C_A, and C_B. J1, R_F, and C_F are often cooled to cryogenic temperatures in Ge detector setups. The circuit works at ±2.6 V power supply, with V_{FET} = 10 V, R_D = 1.2 kΩ, C_F = 0.4 pF, R_F = 1 GΩ, C_M = 1.4 pF, and I_R ~ 560 nA. The latter parameter yields a ramp slope of ~1.4 V/μs. A 15 pF capacitor has been used to simulate the detector. The impulse response of the amplifier shows a 10%-90% rise time of 12 ns. The input-referred series and parallel noises e_n and i_n are as low as 1.1 nV/Hz$^{1/2}$ and 4.2 fA/Hz$^{1/2}$ including the noise contribution of 4.08 fA/Hz$^{1/2}$ due to R_F.
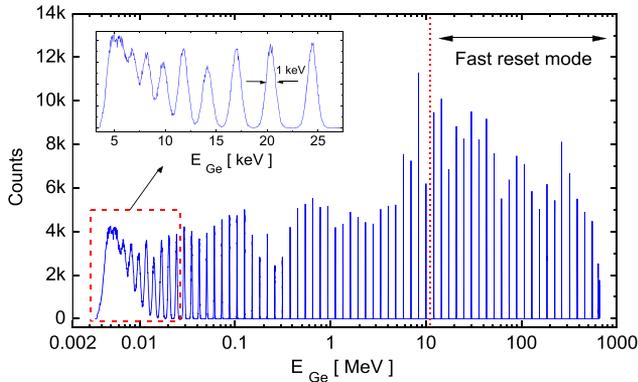
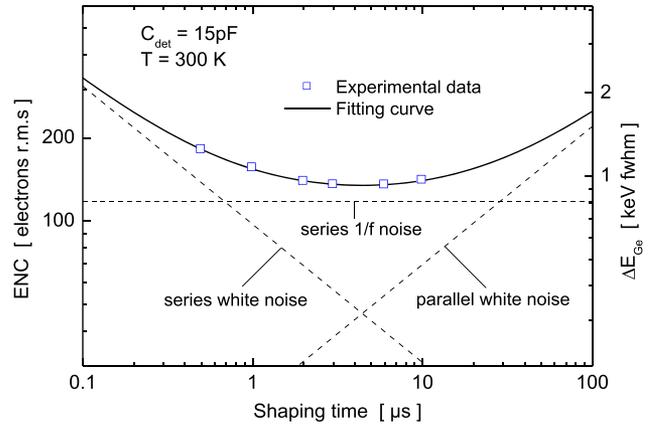FIG. 3. Spectrum of pulser lines distributed over a broad range of amplitude values spanning five orders of magnitude in energy.

FIG. 4. Equivalent noise charge of the integrated preamplifier as working in the low-noise under-threshold regime.

The ASIC is realized in the low-noise AMS C35 0.35 μm CMOS technology. In Fig. 2(b), a picture of the preamplifier is shown. Area occupancy is 900×110 μm^2 excluding the bonding pads. Power consumption of the ASIC is ~20 mW.

In order to test the spectroscopic performance of the system, we injected input charge signals by providing step voltage pulses to a 1 pF calibrated capacitance connected to the preamp input, in a wide range from 0.28 fC to 36 pC, i.e., from 5 keV to 650 MeV in terms of particle energy in Ge detectors, and analyzed the output signals on a pulse-by-pulse basis. In Fig. 3, the obtained spectrum is shown. The negative threshold of T1 was set at -1.38 V, corresponding to an event energy of ~10 MeV.

Signals of amplitude smaller than 10 MeV have been processed conventionally using a quasi-Gaussian spectroscopy amplifier set at 6 μs shaping time, a baseline restorer, and a pulse height analyzer, obtaining an ENC (Equivalent Noise Charge)[9] of ~135 r.m.s. electrons, i.e., ~1 keV fwhm in Ge detectors, which is adequate in most applications.

Signals of amplitude larger than 10 MeV, instead, have been processed using the new fast-reset technique by analyzing the width of comparator signals V_{CMP}. Note that the X-axis scale in Fig. 3 is logarithmic; the amplitudes of the pulser lines are arbitrarily distributed on an exponential basis in such a way to appear equally spaced along the X-axis. The relation of the measurement vs Q is linear in both working regimes within ±0.3%. The spectrum of Fig. 3 spans over five orders of magnitude, which yields an ultra-wide linear range of 102 dB. The low-energy tail in the spectrum is due to the increasing density of lines at lower energies, which yields an increased overlap of the line tails to the neighbor lines. In Table I, the width of a few spectrum lines obtained in the fast-reset regime are shown. It can be seen that the resolution is way

better than 0.1%, which is very adequate for high-resolution spectroscopy of charge signals from semiconductor detectors.

In Fig. 4, the ENC of the preamp is shown in the 0.5–10 μs shaping time range. The typical fitting curve is also shown in the solid line together with the three dominant noise contributions as disentangled from the data. From these data, we can derive quantitatively the spectral densities of the series and parallel noises e_n and i_n shown in Fig. 2(a), as described in Ref. 15, obtaining a white component of the series noise of 1.1 nV/Hz$^{1/2}$, a white component of the parallel noise of 4.2 fA/Hz$^{1/2}$, and a 1/f-noise coefficient A_f of 2.5×10^{-13} V^2. Such a relatively large value of A_f may be interpreted and improved as shown in Ref. 16.

The analytical study of the noise in the fast-reset mode is not straightforward and will be carried out elsewhere.

TABLE I. Width of spectral lines in the fast-reset regime.

Energy (MeV)	fwhm (MeV)	σ (%)
20.8	0.0444	0.090 69
154	0.0577	0.015 88
384	0.1657	0.018 31
552	0.2008	0.015 44

[1] A. Pullia, F. Zocca, G. Pascovici, and D. Bazzacco, Rev. Sci. Instrum. **79**, 036105 (2008).
[2] J. G. Rogers, M. S. Andreaco, C. Moisan, and I. M. Thorson, Nucl. Instrum. Methods Phys. Res., Sect. A **413**, 249 (1998).
[3] A. Pullia, G. Pascovici, B. Cahan, D. Weisshaar, C. Boiano, R. Bassini, M. Petcu, and F. Zocca, in *IEEE Symposium Conference Record Nuclear Science* (IEEE, Rome, Italy, 2004), Vol. 3, p. 1411.
[4] G. Pascovici, A. Pullia, F. Zocca, B. Bruyneel, and D. Bazzacco, WSEAS Trans. Circuits Syst. **7**, 470 (2008).
[5] F. Zocca, A. Pullia, D. Bazzacco, and G. Pascovici, IEEE Trans. Nucl. Sci. **56**, 2384 (2009).
[6] V. Radeka, IEEE Trans. Nucl. Sci. **17**, 269 (1970).
[7] D. A. Landis, N. W. Madden, and F. S. Goulding, IEEE Trans. Nucl. Sci. **45**, 805 (1988).
[8] D. A. Landis, C. P. Cork, N. W. Madden, and F. S. Goulding, IEEE Trans. Nucl. Sci. **29**, 619 (1982).
[9] W. M. C. Sansen and Z. Y. Chang, IEEE Trans. Circuits Syst. **37**, 1375 (1990).
[10] S. Tedja, J. Van der Speigel, and H. H. Williams, IEEE J. Solid-State Circuits **30**, 110 (1995).
[11] C. D. Boles, B. E. Boser, B. H. Hasegawa, and J. A. Heanue, IEEE J. Solid-State Circuits **33**, 733 (1998).
[12] G. Bertuccio, P. Gallina, and M. Sampietro, Electron. Lett. **35**, 1209 (1999).
[13] G. Bertuccio and S. Caccia, Nucl. Instrum. Methods Phys. Res., Sect. A **579**, 243 (2007).
[14] E. Gatti, P. F. Manfredi, M. Sampietro, and V. Speziali, Nucl. Instrum. Methods Phys. Res., Sect. A **297**, 467 (1990).
[15] G. Bertuccio and A. Pullia, Rev. Sci. Instrum. **64**, 3294 (1993).
[16] A. Pullia and G. Bertuccio, Nucl. Instrum. Methods Phys. Res., Sect. A **380**, 1 (1996).